Antenna Radiation Characterization for On-Body Communication Channel Using Creeping Wave Theory

Zhongkun Ma[1], Julien Sarrazin[1], Luca Petrillo[2], Theodoros Mavridis[2],

Philippe De Doncker[2] and Aziz Benlarbi-Delaï[1]

[1] (Université Pierre et Marie Curie, UPMC): L2E Department, F-75005 Paris, France, mazhongkun@gmail.com, julien.sarrazin@upmc.fr, aziz.benlarbi_delai@upmc.fr

[2] (Université Libre de Bruxelles, ULB): OPERA Department-Wireless Communications Group, B-1050 Brussels, Belgium, luca0702@gmail.com, tmavridi@ulb.ac.be, pdedonck@ulb.ac.be

***Abstract*—Creeping wave theory is re-visited for BAN (Body Area Network) channel modeling. The formulation takes the characteristics of both antenna and human tissues into account. The field density at a certain distance from the radiating antenna can be directly determined by input power and on-body antenna gain. It is observed that the complicated on-body antenna gain measurement can be replaced by measuring antenna gain above infinitely large PEC (perfect electric conductor) plane to determine field density. Using time gating technique, the antenna gain above infinitely large PEC can be obtained by measuring continuous field on finitely large PEC, which is much easier to use in practice. The whole concept is validated through CST Microwave Studio. A very good agreement between the analytical model and full-wave simulation results is achieved.**

***Index Terms*—Body area network (BAN), channel modeling, antena characterization, creeping wave theory.**

I. INTRODUCTION

The demand of continuous health monitoring for elders and patients combined with on-going development of low-power devices and miniaturization of wireless application has triggered a new generation of wireless networks, which is known as body area network (WBAN) [1-3]. In order to optimize the battery life for electronics devices, it is crucial to know all the propagation mechanisms in BAN channel to determine the link budget. A channel model can be mainly categorized as statistical and deterministic approaches. The statistics approach models the characteristics of the path loss due to body movements [2], [3], which is out of the scope of this paper. This paper focuses on deterministic approach, which leads to insights regarding on-body propagation.

The first theoretical treatment for on-body deterministic channel model was presented in [4], where author introduces a four-layer Norton wave formulation covering the frequency range from 1 GHz to 11 GHz for BAN. Later on, this Norton wave approach was validated at 60 GHz too [5]. In addition to this approach that models the body surface as a planar multilayer structure (stratified Skin/Fat/Muscle structure), creeping wave theory treats the body as a dielectric cylinder. The advantage of the later approach is allowing predicting path loss of the communication link when two transceivers are located on opposite sides of the body, or when there is no line-of-sight.

Creeping wave formulations, originally intended to be applied to a Hertzian dipole radiation around the bending earth surface in [6], is firstly employed for BAN channel modeling at 2.45 GHz in [7]. As Norton wave approach, it can also be employed for BAN channel modeling at 60 GHz [8]. The dipole moment source in [7] was replaced to be a PIFA antenna in [9], which successfully establishes a link between the injected power, on-body antenna gain and field density. A drawback of creeping wave formulation approach is that it requires on-body antenna gain measurement, which is very difficult in practice as pointed out in [9], where only simulated gain in full-wave solver was employed to estimate the on-body antenna gain.

From the creeping wave formulation, it is clearly observed that the knowledge of the radiation pattern of antennas on an infinitely large PEC is sufficient to determine its radiated field on a lossy dielectric cylinder. Using time gating technique, the antenna is not necessary to be placed on infinitely large PEC. The goal of this paper is consequently to validate this approach using small monopole antennas as example using CST Microwave Studio.

II. CREEPING WAVE MODEL FORMULATION

The on-body communication channel investigated here considers two sensors closely located on the human body surface. For simplification reason, the human body is modeled as a homogeneous cylinder as illustrated in Fig.1. Some researchers treat the human body as elliptical cylinder as well [10], [11]. Our proposed antenna characterization approach can also be employed with these elliptical cylinder assumptions. Both PEC and dielectric cases are investigated at 2.45 GHz, where a relative permittivity of 50 and conductivity of 1.7 S/m is considered for the dielectric [12]. The cylinder radius r is chosen as 10 cm in order to model human's head.

It is well known that the horizontal component (i.e. tangential to the body surface) of the electric field suffers more attenuation compared to the vertical component (i.e. normal direction to the body surface) [4]. Therefore, only the vertical polarization is considered throughout this paper.

The electric field radiated by a source at a distance ρ_s over a cylinder of radius r can be written as a sum of clockwise and anti-clockwise propagating waves (see Fig.1):

$$E_{total}(\rho_s) = E(\rho_s) + E(2\pi r - \rho_s) \quad (1)$$

each wave can be then expressed as:

$$E(\rho_s) = E_0(\rho_s) W(\rho_s, r, \underline{\varepsilon_r}, h_{TX}, h_{RX}) \quad (2)$$

where E_0 is the inverse distance field, which corresponds to the electric field radiated by an antenna above a conducting plane in free space. $E_0(\rho_s)$ can be written as:

$$E_0(\rho_s) = \sqrt{\frac{\eta_0}{2\pi}} \frac{\sqrt{p_{in} G}}{\rho_s} e^{-jk_0\rho_s} \quad (3)$$

where P_{in} is the antenna's input power, G is the antenna gain over infinitely large conducting plane, ρ_s is the distance between the source and the observation point, k_0 is the wave number, η_0 is the vacuum wave impedance. W is the attenuation function that takes into account the losses due to the human tissue's complex permittivity $\underline{\varepsilon_r}$ and the curvature of the surface. h_{TX} (h_{RX}) stands for the distance between the body surface and transmit (receive) antenna. Using W, the creeping wave formulation transforms the radiated field on a flat surface to the radiated field around the circular section of a cylinder by a weighting function as demonstrated later. The detail of W expression is given in [8], [9].

Eq. (2) and (3) implies that complicated on-body antenna gain measurements could be substituted by measuring antenna gain above infinitely large PEC plane. This is this aspect that is proposed to be investigated in the following.

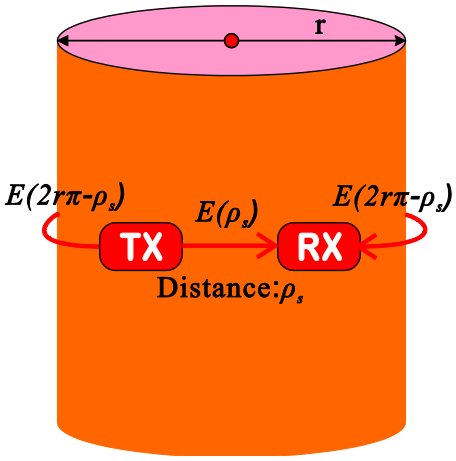

Fig.1. Geometrical assumption of the human body

III. Concept Validation

A monopole antenna (4.5 mm height with 10x10 mm^2 PEC ground plane and excited by 0.5 mm delta gap current source) is chosen as antenna under test (AUT). The simulated result from CST frequency domain solver is plotted in Fig.2, together with the analytical result based on creeping wave theory.

For the simulation case, AUT is located on the cylinder surface in the normal direction to generate vertical polarization along the cylinder surface. Full-wave simulation is employed to obtain the radiated field around the cylinder, which is time consuming.

For the creeping wave analytical case, the gain of AUT above infinitely large PEC plane is firstly simulated in CST, which is much faster than the previous full-wave simulation case. Then this simulated gain is used in the analytical model described in Eq. (1) to (3) to obtain the radiated field. The CST simulated azimuthal gain ($\theta = 90^o$) of AUT is 1.61 dBi and 4.76 dBi when locating in free space and above infinitely large conducting plane, respectively. The later one is employed in E_0 formulation in Eq. (3) to determine the radiated field of the monopole antenna above the infinitely large PEC plane. No normalization is then performed to compare the radiated E-field intensity between full-wave and analytical results.

AUT is located at $\rho_s = 0$ and measured field is from $\rho_s = 0$ to $\rho_s = 2\pi r \approx 628$ mm. For comparison purpose, AUT is assumed to be perfectly matched and consequently accept an identical power of 1 Watt for all the tested cases. The simulated field and analytical field are total E-field in Cartesian coordinate system and r-component E-field (other components being negligible) in cylinder coordinate system, respectively.

As shown in Fig.2, a very good agreement between analytical and CST results is observed. It has to be emphasized again that there is no normalization for all the cases and yet absolute intensity values agree. It is also observed the E-field difference between PEC and dielectric cylinder case is only about 2.5 dB by comparing (a) and (b) in Fig.2. Similar result is also observed by replacing the monopole antenna to patch antenna. In order to reduce the discrepancy of the numerical method [13], these above cases were re-simulated in CST with the time domain solver and a similar conclusion has been obtained.

IV. Antenna Gain Measurement By Time Gating Technique

As shown in the previous section, the complicated on-body antenna gain measurement can be substituted by measuring antenna gain above infinitely large PEC. Unfortunately, measuring the antenna gain above infinitely large PEC is still not practical. However, by using time gating technique, the antenna gain above infinitely large PEC can be obtained from measurements performed on finite size good conductor plane.

To illustrate the concept, the AUT, which is the same one as in previous section, is placed above a PEC plane with size of 1200 x 1200 mm^2 as shown in Fig.3. To measure the propagating electric field radiated by the source, perfect probes are used in simulation in order to firstly assess the approach. Five E-field probes are placed on the PEC surface

along a common axis to determine the influence of their position while calculating the antenna gain obtained with time gating. All of them are separated by a distance d = 50 mm. The nearest and farthest ones to the radiating source are 50 mm and 250 mm, respectively.

Recorded E-fields are plotted together in Fig. 4(a) for each probe in the time domain. The position of recorded pulses in time is consistent with the location of each probe with respect to the radiated. The reflected wave from finite-size PEC plane's edges shows up between 4 ns and 6 ns. These reflected waves do not exist if the size of the ground PEC is infinitely large. Consequently, a time gating is performed such that only the response up to 3 ns remains. All reflections occurring after 3 ns are consequently filtered. The truncated time domain signal is transformed to frequency domain by Fourier transformation, so $E_0(\rho_s)$ is obtained. Based on Eq.(3), the antenna gain can be then calculated by:

$$G = \frac{2\pi}{\eta_0}\frac{(|E_0(\rho_s)|\times\rho_s)^2}{p_{in}} = \frac{1}{60}\frac{(|E_0(\rho_s)|\times\rho_s)^2}{p_{in}} \qquad (4)$$

In order to see if the chosen gating window will influence the results, the gating window varies from 2.5 ns to 6 ns by a step of 0.034 ns. All the results are summarized in Fig.4 (b). The solid line and dot line present the antenna gain by time gating technique when placing AUT on infinitely large and finitely large PEC (size is 1200 x 1200 mm^2), respectively. Ideally they should be identical if the reflected wave of the finite PEC case can be completely removed by choosing a proper gating window. As shown in Fig.4 (b), the result of infinitely large PEC case is identical no matter what gating window is chosen, because there is no reflected wave, which can be treated as the reference for finite PEC case to achieve.

To obtain correct antenna gain using Eq.(4), the probe needs to be placed in the far field region. For the nearest probe, it obtains a 4.15 dBi gain (infinite PEC case), which is 0.61 dB less than that of far field approach (4.76 dBi). One possible reason is this probe is too near to the source and still in the near field of the antenna. As a result, it implies that for very low frequency, the size of the finite PEC needs to be very large. As the distance between the probe and the source increases, the obtained gain increases as well. When the distance increases to 250 mm, the probe is probably in the far field of the antenna because the gain obtained by time gating technique is almost identical as that of far field approach for infinitely large PEC case. To see it clearly, the antenna gain obtained by different probes' positions is plotted in Fig. 5, where gating window is fixed as 2.5 ns for each probe. It is clear that as the distance between the probe and the source increases, the obtained gain increases and starts to converge to the far field gain around 250 mm when the probe is in the far field.

If gating window is chosen between 2.5 ns and 3.5 ns, antenna gains obtained from the finite PEC cases match those from infinitely large PEC cases very well for all the probe positions except the one at 250 mm from source. This is because at 250 mm distance, the probe is closed to the edge of the finite PEC, the incident and reflected wave cannot be distinguished at that location. As gating window increases from 3.5 ns to 6 ns, the obtained gain from the finite PEC cases oscillates because the contribution of reflected waves is not entirely canceled.

Calculated radiated field over cylinder using creeping wave formulation with antenna gain obtained by time gating technique above finite PEC is also plotted Fig. 2. The antenna gain is determined by the probe placed 200 mm away from the source and the gating window is chosen as 2.5 ns. A very good agreement is observed. This agreement proves the concept that when employing creeping wave theory for BAN channel modeling, the complicated on-body antenna gain measurement can be replaced by measuring antenna gain above finite PEC, which is much easier to use in practice.

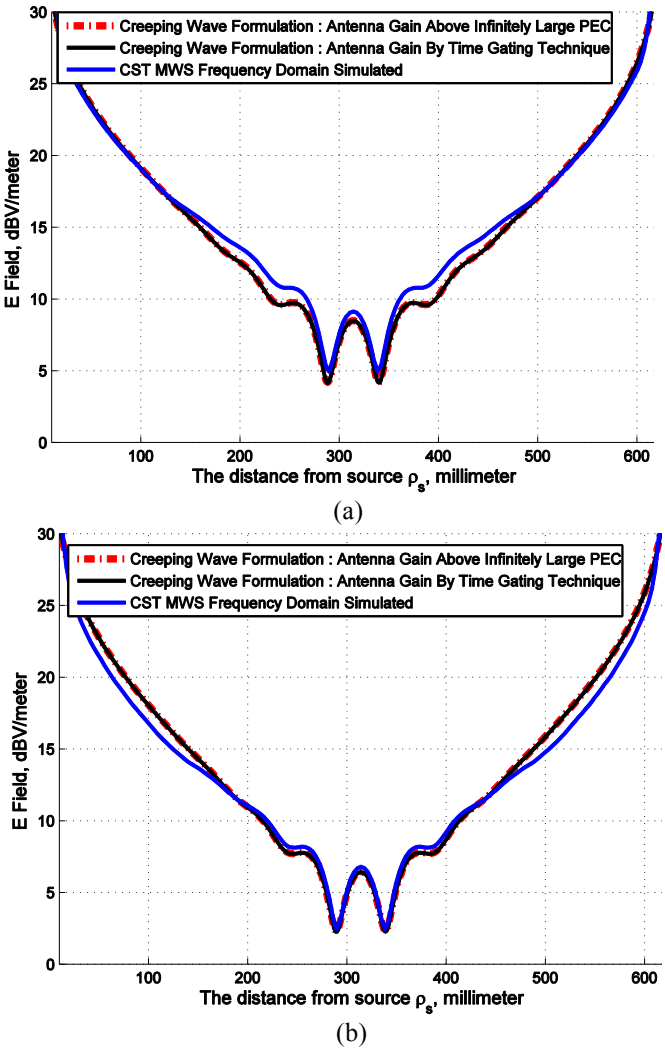

Fig.2. Analytical and simulated E-Field radiated by a monopole antenna (5mm height with 10x10 mm^2 ground plane) around a) PEC cylinder and b) dielectric cylinder (relative permittivity 50 and conductivity 1.7 S/m) with 10 cm radius. Note: These CST simulated results are obtained by Frequency Domain Solver.

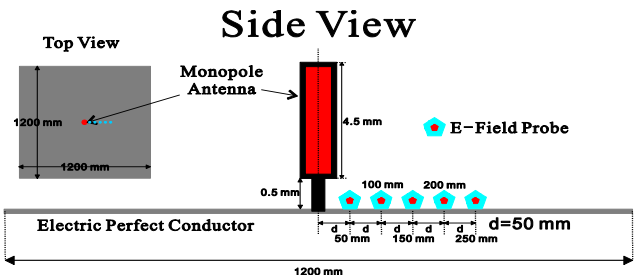

Fig.3. Simulation setup for gain measurement by time gating technique.

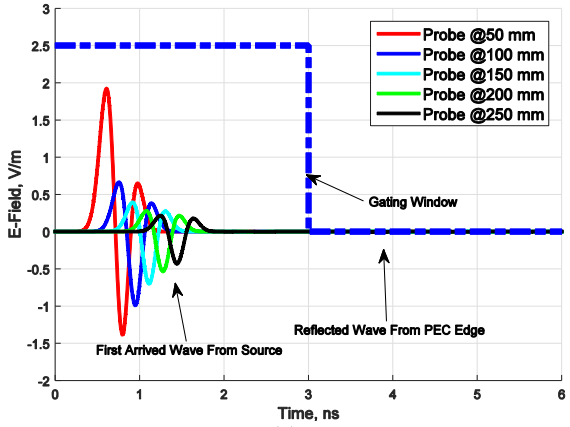

(a)

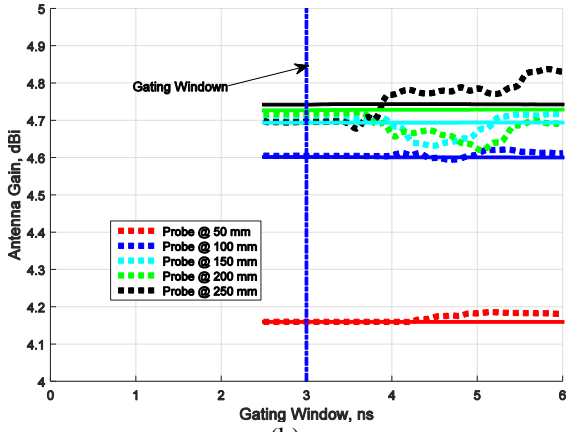

(b)

Fig.4. a) The measured propagated field density versus time by the five probes and b) The antenna gain above infinitely large PEC measured by time gating technique.

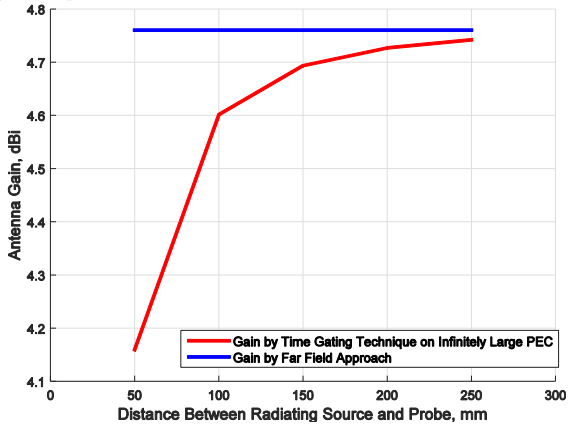

Fig.5.The antenna gain above infinitely large PEC measured by time gating technique (gating window is 2.5 ns) at different probes' positions.

V. Conclusion

Creeping wave formulation is re-visited for body area network channel modeling. This paper showed that the required complicated on-body antenna gain measurement can be replaced by measuring antenna gain above a finite PEC plane. A very good agreement between the analytical model and full-wave simulation results is achieved. It was also noticed that the probe to the source distance should be carefully chosen such that measurements are performed in far-field and that reflection from PEC's edges can be distinguished from incident. Perspectives of this work are now to validate the whole concept by experiment.

VI. Acknowledgement

This work was performed within the Labex SMART supported by French state funds managed by the ANR within the Investissements d'Avenir programme under reference ANR-11-IDEX-0004-02.

VII. References

[1] S.L. Cotton, R. D. Errico, and C. Oestges. "A Review of Radio Channel Models for Body Centric Communications.", *Radio Science*, vol. 49, no.6, pp.371–388, 2014

[2] Q. Wang, T. Tayamachi, I. Kimura, J. Wang "An on-body channel model for UWB body area communications for various postures." *IEEE Trans. Antennas Propagat.*, vol.57, no.4, pp.991-998, 2009

[3] A. Fort, C. Desset, P. de Doncker, P. Wambacq, and L. Van Biesen, "An ultra-wideband body area propagation channel model—From statisticals to implementation," *IEEE Trans. Microw. Theory Tech.*, vol. 54, no. 4, pp. 1820–1826, 2006.

[4] A. Lea, P. Hui, J. Ollikainen, and R. G. Vaughan, "Propagation between on-body antennas," *IEEE Trans. Antennas Propag.*, vol. 57, no. 11, pp. 3619–3627, 2009

[5] N. Chahat, G. Valerio, M. Zhadobov, and R. Sauleau. "On-body propagation at 60 GHz." *IEEE Trans. Antennas Propag.*, vol. 61, no. 4, pp. 1876-1888, 2013

[6] V. Fock. "Diffraction of radio waves around the earth's surface", *Acad. Sci. USSR. J. Phys.*, vol. 9, pp.255 -266, 1945

[7] G.A. Conway, W.G. Scanlon, S.L. Cotton, M.J. Bentum. "An analytical path-loss model for on-body radio propagation," *URSI Int. Electromagnetic Theory (EMTS) Symp.* pp.332-335, 2010

[8] L. Petrillo, T. Mavridis, J. Sarrazin, D. Lautru, A. Benlarbi-delai, P. De Doncker. "Analytical Creeping Wave Model and Measurements for 60 GHz Body Area Networks," *IEEE Trans. Antennas Propagat.*, vol.62, no.8, pp.4352-4356, 2014

[9] T. Alves, B. Poussot, J.M. Laheurte. "Analytical Propagation Modeling of BAN Channels Based on the Creeping-Wave Theory," *IEEE Trans. Antennas Propagat.*, vol.59, no.4, pp.1269-1274, 2011

[10] R. Chandra and A. J. Johansson, "An elliptical analytic link loss model for wireless propagation around the human torso," *Proc. 6th Eur. Conf. Antennas Propag.*, , pp. 3121–3124.

[11] R. Chandra and A. J. Johansson, "An analytical link-loss model for on-body propagation around the body based on elliptical approximation of the torso with arms' influence included," *IEEE Antennas Wirel. Propag. Lett.* , vol. 12 , pp. 528 – 531, 2013

[12] C. Gabriel, "4-Cole-Cole analysis on compilation of the dielectric properties of body tissues at RF and microwave frequencies," Brooks Air Force Tech. Rep. AL/OE-TR-1996-0037, 1996 [Online]. Available: http://www.fcc.gov/fcc-bin/dielec.sh

[13] A. Vasylchenko , Y. Schols , W. De Raedt and G. A. E. Vandenbosch "Quality assessment of computational techniques and software tools for planar-antenna analysis", *IEEE Antennas Propag. Mag.*, vol.51, no.1, pp.23 -38, 2009